Journal of Materials Chemistry A

Accepted Manuscript

ROYAL SOCIETY OF CHEMISTRY

www.rsc.org/materialsA

Journal Name

ARTICLE

Facile Method to Synthesize Carbon Layer Embedded into Titanium Dioxide Nanotubes with Metal Oxide Decoration for Electrochemical Applications

Received 00th January 20xx,
Accepted 00th January 20xx

DOI: 10.1039/x0xx00000x

www.rsc.org/

Yan-Yan Song,[a] Ya-Hang Li,[a] Jing Guo,[a] Zhi-Da Gao,*[a] and Ying Li*[b]

We report a facile and economical method to form carbon layer embedded into self-organized titanium dioxide nanotubes (C/TiO_2 NTs)with a double-walled morphology by one-step pyrolysis method. The carbon precursors are the organic electrolyte remained in nanotube channels during the anodic growth of TiO_2 nanotubes(TiO_2 NTs). By combining layer-by-layer (LBL) technique with galvanic displacement reaction, noble oxide nanomaterials can be anchored onto the nanotubes. Using RuO_2 as a model, the formed TiO_2/C-RuO_2NTs ternary compositeexhibits significantly enhanced pseudocapacitor properties with capacitance value up to 14 times higher than bare TiO_2NTs and a high utilization efficiencyof RuO_2 (1089 F g^{-1}). Additionally, the composite shows a satisfied long-term cycling stability with only 7% decrease after 500 cycles. This strategy opens up a platform to enhanced functionality of TiO_2NTs for novel electrochemical applications.

Introduction

Electrochemical capacitors (ECs), sometimes called supercapacitors or ultracapacitors, have attracted huge attentions as one of the most popular energy storage devices, due to their high power density, long cycle life and very short charging/discharging times.[1-3]Supercapacitors can be classified into two categories according to their charge storage mechanism: electric double-layer capacitors (EDLCs) and pseudocapacitors (so-called redox supercapacitors). EDLCs work based on electrostatic charge storage onto electrode surface by reversible adsorption of electrolyte ions. For EDLCs, carbon and carbon-based materials have been used widely as the electrode materials because of their good electrical conductivity, large high surface area, and satisfied chemical stability.[4-7] Nevertheless, the specific capacitanceof EDLCs is quite small due to the charge accumulation in electrical double layer.[8-11] On the other side, the specific capacitance of pseudocapacitors are originated from the Faradaic redox reactions of electroactive materials. Metal oxides and conducting polymers, such as MnO_2, RuO_2, Fe_3O_4, V_2O_5, TiO_2, NiO, polypyrrole, polyaniline etc. are usually used as the active pseudocapacitor materials.[12-18] As one of the most potential pseudocapacitor materials, RuO_2 has a theoretical specific capacitance of 1400 to 2200 Fg^{-1}.[19] However, most of the reported works can only reach a high mass specific capacitance of 600 to 750 Fg^{-1}. And the high cost is another key point that restricts the bulk commercial use of RuO_2. Thus, it's important to explore an ideal electron-conductive substrate for RuO_2 loading, and significantly improve the utilization efficiency of the valuable RuO_2.

Electrodes prepared from oriented nanotube arrays, contacted with the current collectors directly, can readily be prepared by electrochemical anodization. In contrast to the random charge transfer between nanoparticles, the aligned perpendicular structure can improve charge transfer properties (directional electron transfer in 1D nanotube). These charge transfer properties make nanotubes (NTs) a good candidate in promoting rapid charge/discharge kinetics. Over the past few years, titanium dioxide nanotube arrays (TiO_2 NTs) have attracted tremendous scientific interests since the first report on the self-organized formation of TiO_2 NTs by electrochemical anodization.[20] The combination of geometric characteristics with the inherent photocatalytic properties provides TiO_2 NTs with great potential in photocatalyst, solar cell, drug releasing, and bioelectronic devices.[21] Furthermore, the high hydrogen evolution potential of TiO_2 in aqueous solution makes TiO_2 NTs a promising negative electrode materials in constructing asymmetrical electrochemical capacitors. As it has been reported that the conductivity of the electrode materials and the electrolytes is one of important factors to determine the power density of an electrochemical capacitor.[22]In recent years, search for efficient method to enhancetheelectron transporthas become one of the most important topics.[23]However, a Schottky barrier layer between the Ti foil (substrate) and the TiO_2 NTs limits the conductivity. This is detrimental especially for the application as electrode materials.[24-26] Herein, to apply TiO_2 NTs as promising materials for electrochemical capacitor, it's important to explore a simple and controllable approach to improve the electrical conductivity of TiO_2 NTs.

Here, we introduce a facile, efficient, and economical approach that is based on introducing a pyrolysis process after

[a] College of Science, NortheasternUniversity, Wenhua Road 3–11, Shenyang,China, E-mail: gaozd@mail.neu.edu.cn
[b] JiangsuProvince Hi-Tech Key Laboratory for Bio-medical Research,School of Chemistry and Chemical Engineering, SoutheastUniversity, Nanjing 210096, China Email: yingli@seu.edu.cn
†Electronic Supplementary Information (ESI) available. See DOI:10.1039/x0xx00000x
‡Yan-Yan Song and Yahang Li contributed equally to this work.

anodization to form double-walled tubes with significantly improved electronic performances. The resultant double-walled layers can be severed as an ideal 3D matrix to anchor noble oxide nanomaterials by combining layer-by-layer (LBL) technique with galvanic displacement reaction between Cu and noble metal ions. In the present work, RuO_2 was selected as a model of noble metal oxide. The formed TiO_2/C-RuO_2NTs ternary composite exhibits a highly enhanced specific capacitanceand long term stability.

Experimental

Sample preparation

Synthesis of "double-walled" TiO_2 nanotube arrays. TiO_2 nanotube layers were prepared by electrochemical anodization of Ti. For this, Ti foils (0.1 mm thickness, 99.6% purity) were firstly degreased by sonication in ethanol, followed by thoroughly rinsing with deionized (DI) water and drying by nitrogen stream. The Ti foils were used as the working electrode, and a platinum gauze served as the counter electrode. After the anodizationin an electrolyte of ethylene glycol (EG) containing 0.135 M NH_4F and 1 M H_2O at 50 V for 6 h, the samples were washed in a bath of DI water for 1 min to remove the organic electrolyte on the sample surface and then annealed in argon (Ar) atmosphere at 450 ^oC for 1 h. To prepare the anatase TiO_2 NTs without carbon grafting, the as-prepared samples were dipped into ethanol for 24 h, and then annealed in air at 450 ^oC for 3 h.

Preparation of TiO_2/C-RuO_2 NTs composites. The as-prepared TiO_2/C NTs were first dipped into a 5% poly (styrene sulfonate) (PSS) solution for 2 h. After rinsed with ethanol thoroughly, the samples were dipped into an aqueous $CuCl_2$ (4 mL, 0.2 M) solution for 12 h and washed carefully by DI water to remove weakly adsorbed Cu^{2+}. This cycle made one bilayer of PSS^-/Cu^{2+} on TiO_2/CNTs, and the decorating cycle was repeated two times. Then, the samples were dipped in $NaBH_4$ aqueous solution (10 mg mL^{-1}) for 1 h. The fresh-prepared TiO_2/C-Cu samples was dried by N_2 stream and immediately incubated in an aqueous $RuCl_3$ solution (860 µM) at 80 ^oC for 12 hours. The resulted samples were treated at 120 ^oC for 1 h in ambient air. This temperature was determined from thermo-gravimetric analysis (TGA, as shown in Fig. S1).

Apparatus

The morphologies were characterized using a scanning electron microscope (SEM Hitachi S4800, Japan) andtransmission electron microscopy (TEM, JEOL 2000).X-ray photoelectron spectra (XPS) were measured on a Perkin–Elmer

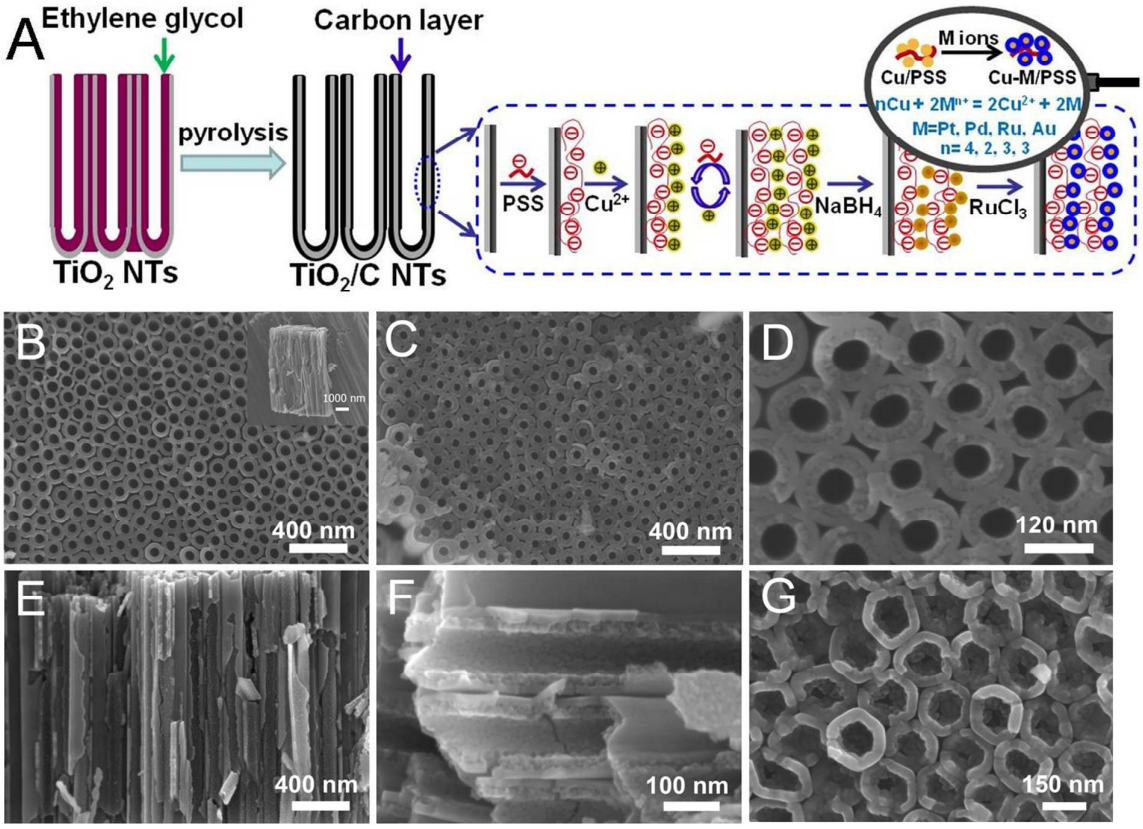

Fig. 1(A) An overview of the process steps to prepare TiO_2/C-RuO_2 NTs from TiO_2NTs. SEM images of bare TiO_2 nanotubes: B) top-view and side-view (inset). SEM images of double-walled C/TiO_2 nanotubes: C) and D) top-view, E) and F) side-view, and G) after nanotubes fracture closed to bottom.

Journal Name

ARTICLE

Physical Electronics 5600 spectrometer using Al K_α radiation at 13 kV as excitation source.The binding energy of Ti 2p signal(458.0 eV) was used as the reference. Thermo-gravimetric analysis was carried out with a TGA (BrukerTG-DTA 2000SA) at arateof10 ^{o}C min^{-1}. The crystallinity and phase of prepared samples were characterized by Raman (LabRAMXploRA, HORIBA JOBIN YVON S.A.S) and XRD (Philips, Guildford, Surrey, U.K.) with a Cu K_α X-ray source. Inductively coupled plasma (ICP) results of the products were determined on an Agilent 7500a ICP-MS analysisinstrument (Agilent Technologies Inc., USA). The nitrolysis of the samples was carried out subsequently with concentrated HNO_3 at 95 ^{o}C for 120 min, H_2O_2 at 95 ^{o}C for 90 min. The reported results of the samples are the average of three replicates. A CHI660D electrochemical workstation (CH Instrument Co., Shanghai) was used to record the electrochemical signals of the samples at ambient temperature (25 ^{o}C). The TiO_2 NTs with 8 mm in electrode diameter acted as the working electrodes. A saturated calomel electrode (SCE) and a Pt sheet were used as the reference and counter electrodes, respectively. The electrochemical performances of the electrodes were characterized by means of cyclic voltammetry (CV) and charge–discharge galvanostatic measurements, with H_2SO_4 (1 M) as electrolyte.

Results and discussion

Fig.1Aillustrates an overview scheme for the process steps applied in this work. Fig. S2presents the as-prepared 'classic'nanotube from a most typicalEG–H_2O–NH_4F electrolyte. A layer of carbon-containing organic electrolyte can be seen in the nanotubes.Fig. 1B shows the tube layers after annealing in air. Itis clear that the tube walls are smooth and clean.The layer thickness is about 5.3 µm.The as-formednanotube layers consist of amorphous TiO_2,and can be convertedto anatase(which provides better conductivity compared to amorphous and rutile crystalline) by annealing at 450 ^{o}C.

When the nanotube layer is annealed in Ar after anodization, the double walledstructure is formed (Fig.1C and D, denoted as TiO_2/C NTs). This annealing process includes the transfer of TiO_2 crystalline from amorphous to anatase, and meanwhile the pyrolysis of carbon precursor (the EG electrolyte remained in the nanotubes during anodization process) at high temperature to grow carbonlayer.In Fig. 1D, the distinction between outer and innerlayers is very evident for the double-walled tubes.The formed inner carbon shell (~10nm thick wall) is tapered from top tobottom (Fig.1E-G), showing the effectiveness of the coating procedure. If the samples are immersed in ethanol after anodization, EGmolecules dissolve into ethanol and diffuse out of nanotubes gradually,resultingin the decrement of carbon precursorconcentration in tube channels. Thus, the thickness of carbon shell (carboncontentin the tubes) can be control.

Raman spectroscopy was applied to study the as-prepared TiO_2/C NTs samples. As shown in Fig.2A, the Raman bands appeared at 399, 519, and 645 cm^{-1} are assigned to anatase modes of TiO_2. The Raman band observed at 1406 cm^{-1} (inset of Fig.2A) is assign to the carbon defected-induced Raman band (D band). And the band observed at1577 cm^{-1} can beattributed to the ordered graphitic structure (G band), which indicates the existence of partly graphitized carbon.

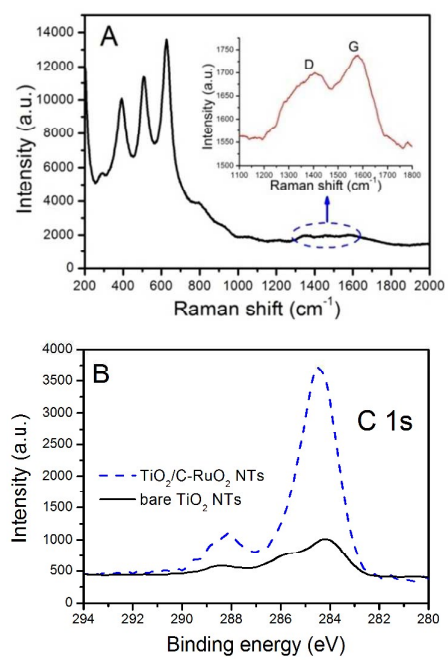

Fig. 2(A) Raman spectra of TiO_2/C NTs, and (B) XPS narrow scan spectra of C 1s for bare TiO_2 NTs and TiO_2/C NTs.

To study the concentration and atomic structure of carbon, XPS measurements were carried out as shown in Fig.2B. For comparison, the bare TiO_2NTs(annealed in air at 450 ^{o}C) was also analysised. The presence of a high amount of carbonfor TiO_2/C NTs confirms the formation of carbon via pyrolysis of the EG (and incorporation) in Ar at high temperature. If the as-formed nanotubes are annealed without the protection of Ar, this process may be accompanied with additionalincorporation

of oxidized carbon species at high temperature by O_2. Thus, the samples is almost carbon free (Note: the peak at 284.3 eVcomes from the naturalcarbon contamination—alwaysobserved for samples transferred in air—is normally present).

Combining layer-by-layer (LBL) technique with sodium borohydride($NaBH_4$) reduction method Cu nanoparticleswere grafted in nanotubes, as shown in Fig. 1A.Galvanic replacement is a facial approach to prepare bimetallic nanomaterials in ambient environment, i.e. Pd, Pt, Au, Ru.[27,28]In this study, $Ru^{3+}$was selectedas a model. Since the standard electrodepotential of the Cu^{2+}/Cu pair (0.34 V) is much lower than that ofRu^{3+}/Ru (0.68 V), the galvanic displacement reaction between Cu and the noblemetal ions can take place easily.Theoretically, Cu(0) can bereplaced completely if the amount of $Ru^{3+}$is controlled more than thatrequired for completely replacing Cu species. Considering thatCu(0) are easy to be oxidized into its oxide form,the fresh-prepared Cu decorated TiO_2/C NTs should be transferred into Ru^{3+} solution immediately to avoid the further oxidation.The resulted TiO_2/C-Ru NTs samples were then oxidized to TiO_2/C-RuO_2 NTs by heating in air. The XRD patterns (Fig. S3) demonstrate the formation of RuO_2 on anatase TiO_2 nanotubes. The XPS spectra (Fig. S4) indicate that the most of Cu (0) issuccessfully formed and then transferred into RuO_2.The EDS mapping images (Fig. S5) further confirm that carbon and RuO_2 are decorated homogemously on the nanotube. The decorated RuO_2 nanoparticles can also be distinguished from high-resolution TEM image (HRTEM, Fig. S2C and S2D) with size ranging from 2 to 4 nm. These RuO_2 nanoparticles are in intimate contact with the carbon and TiO_2 support, and the lattice fringes of both partly graphitized carbon and TiO_2 can be clearly identified in Fig. S2D. The lattice constant of about 0.24 nm is in agreement with the spacing of graphite (112) lattice planes and the lattice spacing of 0.35 nm is consistent with the anatase TiO_2 (101) lattice planes.

To explore the application of this novel design, the electrochemical performances of the as-prepared TiO_2/C-RuO_2 NTs electrodes were further studied. Fig.3A shows the CV results of the electrodes in 1 M H_2SO_4 at a scan rate of 5 mVs^{-1}. The cycling potential window is confined between 0.0 and 0.8 V to avoid the H_2 evolution at lower potentials, and the O_2 evolution at higher potentials. As comparison, the specific capacitance values of TiO_2NTs, TiO_2-RuO_2NTs, and TiO_2/C NTs have also been investigated. In Fig.3A, the severelydistorted CV shapes of pure TiO_2NTs and TiO_2/C NTs indicate their intrinsicallypoor electrochemical capacitance property. The currents of the TiO_2-RuO_2NTs and TiO_2/C-RuO_2NTs electrodes increase significantly and exhibit one pair of wide redox peaks that are indicative of a typical pseudocapacitivebehavior of RuO_2. In this study, the second PSS-Cu^{2+} bilayers in LBL process were chosen for RuO_2 decoration based on the electrochemical currents in Fig. S6. The specific capacitanceof the as-formed electrodes was calculated according to the following equation:[29]

$$C = \frac{Q}{\Delta V} = \frac{S}{2\nu \times m \times \Delta V} \qquad (1)$$

where C (Fg^{-1}) is the specific capacitance, Q is the voltammetric charge, ΔV is the width of potential window, ν is the scan rate, S is the integration area of cyclic voltammetic, and m is the mass of the electrode materials (or mass of active materials). Based on the CV curves in Fig. 3A, the TiO_2/C-RuO_2 NTs electrode shows a specific capacitance of 31.82 Fg^{-1}. This value is higher than the results from TiO_2NTs (2.28 Fg^{-1}), TiO_2/C NTs (2.77 Fg^{-1}), and TiO_2/RuO_2NTs (20.64 Fg^{-1}) at the same scan rate. The capacitance value of TiO_2/C-RuO_2 NTs is up to 14 times higher than the bare TiO_2NTs. The loading of Ru in the TiO_2/C-RuO_2 NTs was further determined by using ICP-MS. ICP result shows that the RuO_2wt% value in TiO_2/C-RuO_2 NTs is 2.68%. The corresponding specific capacitance of the TiO_2/C-RuO_2 NTs is 1089 Fg^{-1} based on the mass of RuO_2 in the sample. This value is very close to that reported previously for hydrous RuO_2 decorated carbon nanofiber electrode (1300 F g^{-1}),[30] and approaching the theoretical specific capacitance value for RuO_2.[19] Clearly, the carbon layer in the double-walled TiO_2/C-RuO_2 NTs is related to this great enhancement. A comparison of TiO_2/C-RuO_2 NTs electrodes with various published results of RuO_2 based supercapacitors is shown in Table 1.These results indicate that the high utilization of RuO_2 for the energy storage is achieved on the double-walled TiO_2/C nanostructure.

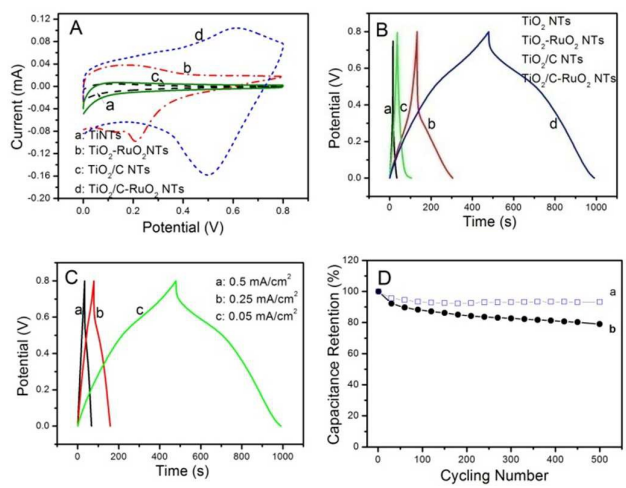

Fig.3(A) Cyclic voltammograms for bare TiO_2 NTs, TiO_2/C NTs, TiO_2-RuO_2 NTs and TiO_2/C-RuO_2 NTs in 1 M H_2SO_4 electrolyte at a scan rate 5 mVs^{-1}. (B) Charge-discharge test for TiO_2 NTs, TiO_2/C NTs, TiO_2-RuO_2 NTs and TiO_2/C-RuO_2 NTs at 0.05 $mAcm^{-2}$. (C) Charge-discharge test for TiO_2/C-RuO_2 NTs at 0.5 $mAcm^{-2}$, 0.25 $mAcm^{-2}$, 0.05$mAcm^{-2}$. (D) Capacitance retention of TiO_2/C-RuO_2 NTs (curve a) and TiO_2-RuO_2 NTs (curve b) electrodes as a function of cycling number.

Fig. 3B exhibits the glavanostatic charge/discharge curves of the TiO_2NTs, TiO_2-RuO_2 NTs, TiO_2/C NTs and TiO_2/C-RuO_2 NTs. Compared to the reference systems (i.e. TiO_2NTs, TiO_2-RuO_2 NTs, TiO_2/C NTs), the RuO_2-C/TiNTscomposite provides

satisfiedcapacitivecharacterswithverysharpresponseand small internal resistance (IR) drop. Based on the discharge

Table 1. A comparison of TiO_2/C-RuO_2 NTs electrodes with various published results of RuO_2 based supercapacitors.

Structure	Preparation approach	Ru loading	Specific capacitance of RuO_2 (Fg^{-1})	Ref
RuO_2-TiO_2 thin film	Electrodeposition	1.4 $mgcm^{-2}$	788	33
RuO_2-TiO_2nanoflowers	Anodic deposition	1 $mgcm^{-2}$	545±35	34
RuO_2-TiO_2nanorods	Heat treatment in N_2	—	687	35
(Ru-Ti)O_2·nH_2ONPs	Hydrothermal process	40 atm%	470	36
RuO_2-Graphene Sheets	Sol-gel process	38.3 wt%	606	37
RuO_2-carbon fabric	Sol-gel process	9.15 wt%	1085	38
RuO_2 nanowire -CNTs	Inkjet-printing process	15 wt%	920	39
RuO_2-carbon nanofiber	H_2O_2 pre-treatment	31 wt%	1300	30
RuO_2/ C/ TiO_2nanotubes	galvanic replacement	2.68 wt%	1089	This work

curve,the specific capacitance was calculated according to following equation:[31]

$$C = \frac{I\Delta t}{m\Delta V} \qquad (2)$$

where C (Fg^{-1}), I (A), Δt (s), ΔV (V) and m (g)are the specific capacitance, discharge current, discharge time consumed in the potential range of ΔV, the potential windows and the mass of electrode material (or mass of active materials), respectively. The specific capacitances calculated from charge-dischargecurves are 4.25, 9.65, 38.27 and 69.18 Fg^{-1} for TiO_2 NTs, TiO_2/C NTs, TiO_2-RuO_2 NTs and TiO_2/C-RuO_2 NTs, respectively. Fig. 3C shows the charge–discharge curves of TiO_2/C-RuO_2 NTs at various current densities. At different current densities, the only comparably small IR drop demonstrates the excellent electrical conductivity of ternary composite samples. Additionally, the TiO_2/C-RuO_2 NTs provide a stable charge-discharge curve, as shown in Fig. S7. The curve is symmetrical with triangular shape and maintains almost the same characteristics.

Long cycling life is another important target for preparing supercapacitorelectrodes. The cyclic lives of the TiO_2/C-RuO_2 NTs and TiO_2-RuO_2 NTs based electrodeshave been continuously tested for up to 500 cycles. As shown in Fig.3D, the TiO_2/C-RuO_2 NT electrode keeps nearly 93% of its capacitance after 500 cycles (curve a), which is much better than that measured from the TiO_2-RuO_2 NTs electrode (79% in curve b). The improved capacitance and remarkable cyclic stability of TiO_2/C-RuO_2 NTs can be attributed to the carbon layer acts as a stable matrix for RuO_2 grafting and thus avoids the accumulation of RuO_2. Furthermore, the good electronic conductivity of nanotubes improves the utilization of RuO_2.

Fig. 4A shows the XPS survey spectra of the as-prepared TiO_2/C-RuO_2 NTs. In addition to the Ti 2p, O 1s and C 1s signals, the distinct Ru XPS signalssuch as 3s, 3p, 3d, 4s, and 4p appear. Fig. 4B gives the comparativeXPS results of the C1s and Ru 3d peaks (~276–292 eV). Dueto the overlap of Ru $3d_{3/2}$ and C1s peaks, the Ru $3d_{5/2}$ peak corresponding to thebinding energyof Ru^{4+} is usually used for identifying the electronic statesof Ru. For the as-prepared TiO_2/C-RuO_2 NTs, the Ru $3d_{5/2}$peak appears at 281.5 eV. The presence of peak at 280.7 eV is arising from metallic Ru in the sample, which suggests the presence of composite Ru-RuO_2 in the TiO_2/C-RuO_2 NTs. Upon electrochemical cyclingin 1 M H_2SO_4 solution for 500 cycles, it's also noted that the Ru $3d_{5/2}$ peak of electrochemical treatment sample shows an increase as compared to the fresh sample; meanwhile, the peak at 280.7 eV corresponding to the metallicRu is decreased after electrochemical cycling treatment. These changes in the high resolution XPS spectra indicate the further oxidation of Ru-RuO_2 composite to RuO_2 during the electrochemical cycling process.[32]

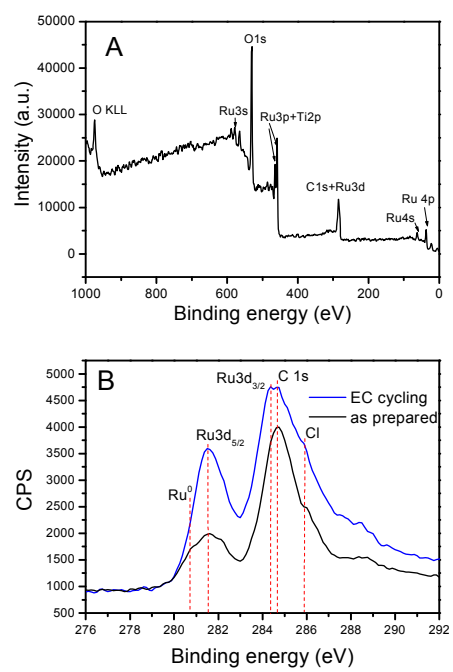

Fig.4(A) XPS survey spectra for TiO_2/C-RuO_2 NTs, and (B) XPS narrow scan spectra of C 1s andRu 3d for the TiO_2/C-RuO_2 NTs before and after electrochemical cycling in 1 M H_2SO_4 solution for 500 cycles.

In order to prove the effectiveness of the galvanic displacement reaction for other metal decoration, TiO_2/C NTs were loaded with Pt nanoparticles based on the displacement reaction between Cu (0) and0.1 M H_2PtCl_6. As shown in Fig. S8, the as-formed TiO_2/C-Pt NTs exhibits satisfiedcatalytic activity for methanol electrooxidation.

Conclusions

A one-step pyrolysis strategy is developed for coating graphite-type carbon layer into TiO_2 nanotubes. This strategy, where one-step pyrolysis of carbon precursors remained in the TiO_2 nanotube channel to form double-walled nanotubular structure, is found to be an efficient and simple attempt to improve the electron conductivity of the TiO_2NTs for further functionality and application. The resulted double-walled nanotubular composite are applied as a 3D scaffold for supercapacitor application with RuO_2 grafting. Owing to the enhanced electronic conductivity and excellent utilization of the RuO_2 nanoparticles, the resulted RuO_2-C/TiNTs ternary composites show ideal capacitive behavior and satisfied long cycling stability for supercapacitor application.

Acknowledgements

This work was supported by the National Natural Science Foundation of China (Nos. 11174046, 21322504, 21275026 and 21005016), the Fundamental Research Funds for the Central Universities (N140505001, N140504006), and the Program for Liaoning Excellent Talents in University (LJQ2013028).

References

1 P. Simon, Y. Gogotsi, *Nat. Mater.*,2008, **7**, 845.
2 Y.Q. Sun, Q. Wu, G.Q. Shi, *Energy Environ. Sci.*,2011, **4**, 1113.
3 D.W. Wang, F. Li, M. Liu, G.Q. Lu, H.M.Cheng, *Angew. Chem. Int. Ed.*,2008,**47**, 373.
4 E. Frackowiak, F. Beguin, *Carbon*,2001, **39**, 937.
5 C. Niu, E.K. Sichel, R. Hoch, D. Moy, H. Tennent, *Appl. Phys. Lett.*,1997, **70**, 1480.
6 M. Endo, T. Maeda, T. Takeda, Y.J. Kim, K. Koshiba, H. Hara, M.S. Dresselhaus, *J. Electrochem. Soc.*,2001, **148**, A910.
7 F. Bonhomme, J.C. Lassegues, L. Servant,*J. Electrochem. Soc.*, 2001, **148**, E450.
8 Y. Huang, J.J. Liang, Y.S. Chen, *Small*,2012, **8**,1805.
9 C.W. Tan, K.H. Tan, Y.T. Ong, A.R. Mohamed, S.H.S. Zein, S.H. Tan, *Environ. Chem. Lett.*,2012, **10**, 265.
10 M.V. Kiamahalleh, S.H.S. Zein, A. Najafpour, S.A. Sata, S. Buniran, Nano,2012, **7**, 1230002.
11 A.G. Pandolfo, A.F. Hollenkamp, *J. Power Sources*,2006, **157**,11.
12 J.M. Miller, B. Dunn, *Langmuir*,1999, **15**, 799.
13 C. Hu, Y. Huang, *J. Electrochem. Soc.*,1999, **146**, 2465.
14 J.K. Chang, W.T. Tsai, *J. Electrochem. Soc.*,2003, **150**, A1333.
15 M. Wu, *Appl. Phys. Lett.*,2005, **87**, 153102.
16 K.R. Prasad, N. Miura, *Appl. Phys. Lett.*,2004, **85**, 4199.
17 T. Cottineau, M. Toupin, T. Delahaye, T. Brousse, D. Belanger, *Appl. Phys. A: Mater.*, 2006, **82**, 599.
18 Y.R. Ahn, M.Y. Song, S.M. Jo, C.R. Park, D.Y. Kim, *Nanotechnology*,2006, **17**, 2865.
19 C.C. Hu, W.C. Chen, K.H. Chang, *J. Electrochem. Soc.*,2004, **151**, A281.
20 M. Assefpour-Dezfulx, C. Vlachos, E.H. Andrews, *J. Mater. Sci.*, 1984,**19**, 3626.
21 A. Ghicov, P. Schmuki, *Chem. Commun.*,2009, **20**, 2791.
22 W. Sugimoto, H. Iwata, K. Yokoshima, Y. Murakami, Y. Takasu, *Phys. Chem. B.*,2005, **109**, 7330.
23 (a) C. Yang, Z. Wang,T. Lin, H. Yin,X.Lü, D. Wan, T.Xu,C. Zheng, J. Lin, F. Huang, X.Xie, M. Jiang,*J. Am. Chem. Soc.*, 2013, **135**, 17831; (b) X.Lü, W. Yang, Z.Quan, T. Lin, L.Bai, L. Wang, F. Huang,Y. Zhao, *J. Am. Chem. Soc.* 2014, **136**, 419; (c) X.Lü , F. Huang, X.Mou, Y. Wang, F.Xu, *Adv. Mater.* 2010, **22**, 3719; (d) X.Lü, X.Mou, J. Wu, D. Zhang, L. Zhang,F. Huang, F.Xu, S. Huang, *Adv. Funct. Mater.;* 2010, **20**, 509.
24 H. Tang, K. Prasad, R. Sanjines, P. E. Schmid, F. Levy, *J. Appl. Phys.*,1994, **75**, 2042.
25 R. Hahn, F. Schmidt-Stein, J. Salonen, S. Thiemann, Y.Y. Song, J. Kunze, V.P. Lehto, P. Schmuki, *Angew. Chem. Int. Ed.*,2009, **48**, 7236.
26 D. Y. Lee, E.-K. Kim, S. J. Yoon, I. Lim, K. Cho, D. V. Shinde, S. A. Patil, W. Lee, Y.-C. Nah, N. K. Shrestha, J. K. Lee, S.-H. Han, *RSC Adv.*, 2014, **4**, 32599.
27 Y.Y. Song, W.Z. Jia, Y. Li, X.H. Xia, Q.J. Wang, J.W. Zhao, Y.D. Yan, *Adv. Funct. Mater.*,2007, **17**, 2808.
28 S. Chen, H. Zhang, L. Wu, Y. Zhao, C. Huang, M. Ge, J. Liu, *Mater. Chem.*,2012, **22**, 9117.
29 X. Liu, P.G. Pickup, *J. Solid State Electrochem.*,2010, **14**, 231.
30 R. Vellacheri, V.K. Pillai, S. Kurungot, *Nanoscale*,2012, **4**, 890.
31 D. M. MacArthur, *J. Electrochem. Soc.*, 1970,**117**, 422.
32 N. Soin, S.S. Roy, S.K. Mitra, T. Thundat, J.A. McLaughlin, *J. Mater. Chem.*,2012, **22**, 14944.
33 C. D.Lokhande, B. O. Park, H. S. Park, K. D.Junga and O. S.Jooa, *Ultramicroscopy*, 2005,**105**, 267.
34 C. C. Hu, H. Y.Guo, K. H. Chang and C. C. Huang, *Electrochem. Commun.*, 2009,**11**, 1631.
35 R. A. Young, R. P. Chong, M. J.Seong and Y. K. Dong, *Appl. Phys. Lett.*, 2007, **90**, 122106.
36 K. H. Chang and C. C. Hu, *Electrochim. Acta*, 2006, **52**, 1749.
37 Z. S. Wu, D. W. Wang, W.Ren,J. P. Zhao, G. M. Zhou, F. Li, H. M. Cheng, *Adv.Funct.Mater.*, 2010,**20**, 3595.
38 X. R. Liu, G. Peter,*J.SolidStateElectrochem.*, 2010,**14**, 231.
39 P. C. Chen, H. T. Chen, J.Qiu, C. W. Zhou, *Nano Res.*, 2010, **3**, 594.

Graphical Abstract

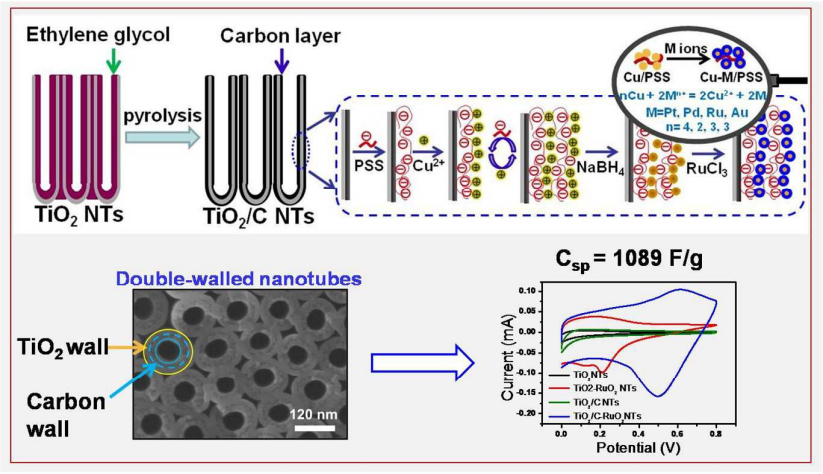

The preparation of carbon layer embedded into titanium dioxide nanotubes with metal oxide decoration for supercapacitors